Available online at www.sciencedirect.com
ScienceDirect
Nuclear Physics B Proceedings Supplement 00 (2014) 1–3
Nuclear Physics B Proceedings Supplement

Measurement of the proton and kaon time-like electromagnetic form factors at high energy with the BABAR detector

V. P. Druzhinin[a,b]

[a]Budker Institute of Nuclear Physics SB RAS, Novosibirsk 630090
[b]Novosibirsk State University, Novosibirsk 630090

Abstract

We have used ISR technique to measure the proton magnetic form factor in the energy region from 3.0 to 6.5 GeV and charged kaon form factor in the range from 2.6 to 7.5 GeV. The proton data clearly indicate that the difference between values of time- and space-like magnetic form factors decreases with increase of energy. The kaon form factor decreases with energy faster than $1/E^2$, approaching the asymptotic pQCD predictions.

Keywords: proton, kaon, electromagnetic form factor

1. Introduction

The proton and kaon time-like electromagnetic form factors are extracted from measurements of the $e^+e^- \to p\bar{p}$ and $e^+e^- \to K^+K^-$ cross sections:

$$\sigma_{p\bar{p}}(m) = \frac{4\pi\alpha^2\beta C}{3m^2}\left[|G_M(m)|^2 + \frac{2m_p^2}{m^2}|G_E(m)|^2\right], \quad (1)$$

$$\sigma_{K^+K^-}(m) = \frac{\pi\alpha^2\beta^3 C}{m^2}|F_K(m)|^2, \quad (2)$$

where m is the $p\bar{p}$ or K^+K^- invariant mass, $\beta = \sqrt{1-4m_{p,K}^2/m^2}$, C is the correction for the Coulomb final state interaction [1, 2]. At high energies the second term in the $p\bar{p}$ cross section is suppressed and the cross section is proportional to the magnetic form factor squared.

The asymptotic behavior of the form factors is predicted in the frame of perturbative QCD [3, 4]

$$F_K = \frac{8\pi\alpha_s f_K}{m^2},\ G_M \propto \frac{\alpha_s^2}{m^4} \quad (3)$$

Previously [5, 6, 7, 8, 9, 10, 11], the proton and kaon form factors were measured up to 4.5 and 5.0 GeV, respectively. It was observed that they decrease in agreement with the pQCD predictions. However, the value of the kaon form factor at 4 GeV exceeds the predictions by about 4 times. For proton, the ratio of the time- and space-like form factors at 4 GeV is about 2 instead of unity expected at high energy. Our goal is to perform measurement at larger energies to answer the question of whether the difference between the prediction and data decreases with energy increase.

The presented analyses are based on the BABAR data sample, 469 fb^{-1}, collected at and near Υ(4S) at the SLAC PEP-II e^+e^- collider. The initial-state radiation (ISR) method is used to measure the cross sections. We study the reactions $e^+e^- \to p\bar{p}\gamma$, $K^+K^-\gamma$. The mass spectrum in the reaction $e^+e^- \to X\gamma$ is related to the cross section for the nonradiative process $e^+e^- \to X$:

$$\frac{d\sigma_{e^+e^-\to X\gamma}(s,m)}{dm} = \frac{2m}{s}W(s,m)\,\sigma_{e^+e^-\to X}(m), \quad (4)$$

where s is the e^+e^- center-of-mass energy. The function $W(s,m)$ is calculated in QED with a high, better than 0.5%, accuracy. In presented analyses simulation of ISR events and calculation of $W(s,m)$ is based on the Phokhara event generator [12], which takes into account next-to-leading order radiative corrections.

The ISR photon is emitted predominantly along the collision axis. The produced hadronic system is boosted against the ISR photon. Due to limited detector ac-

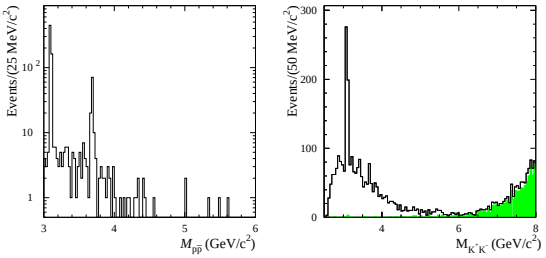

Figure 1: The $p\bar{p}$ (left) and K^+K^- (right) invariant-mass spectra for selected data $p\bar{p}\gamma$ and $K^+K^-\gamma$ candidates. In the K^+K^- mass spectrum, the shaded histogram shows events with at least one identified muon candidate.

ceptance the low-mass region can be studied only with ISR photon emitted at a large angle (LA) and detected. The previous BABAR results on the proton and kaon form factors [10, 11] were obtained using the LA ISR method. Above 3 GeV statistics can be significantly increased by using ISR events with undetected photon emitted at a small angle (SA). Here we present the recent SA ISR measurement for $e^+e^- \to p\bar{p}$ [13] and preliminary SA ISR results for $e^+e^- \to K^+K^-$.

2. Event selection

We select events with two tracks of opposite charge originating from the interaction region, having the polar angle in the range (25.8°–137.5°) and identified as protons or kaons. Further selection are based on two parameters: the transverse momentum (p_T) of the proton or kaon pair and the missing mass ($M_{\rm miss}$) recoiling against it. We require $p_T < 0.15$ GeV/c and $|M^2_{\rm miss}| < 1$ GeV$^2/c^4$.

Due to the energy asymmetry of the e^+e^- collisions at PEP-II (9-GeV e^- and 3.1-GeV e^+) the average proton (kaon) momenta are strongly different in events with ISR photon emitted along the positron and electron beam directions, and are about 5 and 2.5 GeV/c, respectively. We reject events with the photon emitted along the positron beam to decrease background arising due to particle misidentification.

The $p\bar{p}$ and K^+K^- invariant mass spectra for data events selected with the criteria described above are shown in Fig. 1. Peaks from J/ψ and $\psi(2S)$ decays are seen in the spectra. In the K^+K^- mass spectrum, the peak near 3.4 GeV/c^2 is due to the decay chain $\psi(2S) \to \chi_{c0}\gamma$, $\chi_{c0} \to K^+K^-$. We do not observe $p\bar{p}$ events with invariant mass above 6 GeV/c^2. The increase in the number of events at masses above 6 GeV/c^2 in the K^+K^- mass spectrum is due to $e^+e^- \to \mu^+\mu^-\gamma$ background. To suppress the muon background we apply the additional condition that none of the kaon candidates is identified as a muon. The shaded histogram in Fig. 1 shows events with at least one identified muon candidate. Muon background prevent us from measuring the $e^+e^- \to K^+K^-$ cross section at energies higher than 7.5 GeV.

3. Background estimation and subtraction

Possible sources of background in the selected samples are other two-body ISR processes, e.g. $e^+e^- \to \mu^+\mu^-\gamma$, ISR processes containing additional neutral particles, e.g. $e^+e^- \to p\bar{p}\pi^0\gamma$, $K^+K^-\pi^0\gamma$, the two-photon processes $e^+e^- \to e^+e^-p\bar{p}$, $e^+e^-K^+K^-$. The backgrounds from the nonradiative processes $e^+e^- \to p\bar{p}\pi^0$ and $K^+K^-\pi^0$, which were the dominant background sources in our LA analyses [10, 11], are strongly suppressed by the condition on the transverse momentum and found to be negligible in the SA analysis.

The two-body ISR background is found to be negligible for $p\bar{p}$ events, and for K^+K^- events with the K^+K^- mass below 5 GeV/c^2. For higher K^+K^- masses the $e^+e^- \to \mu^+\mu^-\gamma$ process is non-negligible. We estimate the numbers of signal and background events by fitting the $M^2_{\rm miss}$ distribution with a sum of signal and background. The distribution for signal events is taken from simulation and is centered at zero. The distribution for $e^+e^- \to \mu^+\mu^-\gamma$ background is obtained using data events with at least one identified muon. The $\mu^+\mu^-\gamma$ distribution is shifted to negative $M^2_{\rm miss}$ values because of the muon-kaon mass difference. Excess of signal events over background is found for $M_{K^+K^-} < 7.5$ GeV/c^2.

ISR events containing a $p\bar{p}$ (K^+K^-) pair plus π^0 mesons are distinguishable by their nonzero values of $M^2_{\rm miss}$ and p_T. However, some events with a small number of neutrals can enter the selected data samples. We use rectangular sideband ($1 < M^2_{\rm miss} < 3$ GeV$^2/c^4$ and $0.15 < p_T < 1$ GeV/c) and a scale factor obtained from MC simulation to estimate background contribution in the signal region ($|M^2_{\rm miss}| < 1$ GeV$^2/c^4$ and $p_T < 0.15$ GeV/c). It is found to do not exceed 5% of $\bar{p}p$ signal events, and lower for K^+K^-.

Most two-photon events have small values of p_T and large values of $M^2_{\rm miss}$. The two-photon background is estimated by scaling the number of data events found in the $M^2_{\rm miss}$ sideband ($M^2_{\rm miss} > 10$ GeV$^2/c^4$). The scale factor is determined using MC simulation of the two-photon process. This background is found to do not exceed 3% of K^+K^- signal events, and even lower for $p\bar{p}$.

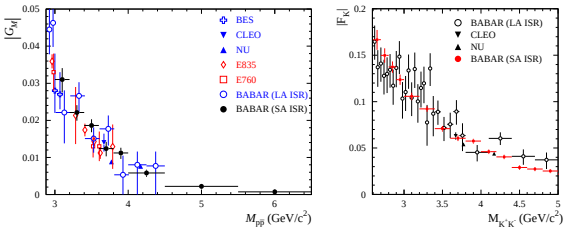

Figure 2: The proton magnetic (left) and charged kaon (right) form factors measured in this analysis [BABAR (SA ISR)] and in other experiments:E760 [5], E835 [6], BES [7], CLEO [8], NU [9], BABAR (LA ISR) [10, 11].

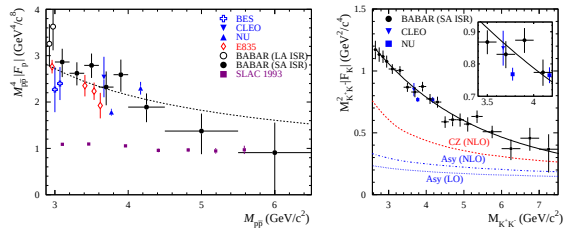

Figure 3: The scaled proton magnetic (left) and charged-kaon form factors measured in this analysis [BABAR (SA ISR)] and in other experiments: E760 [5], E835 [6], BES [7], CLEO [8], NU [9], BABAR (LA ISR) [10]. Points denoted by 'SLAC 1993" represent data on the space-like magnetic form factor obtained in ep scattering [14]. The curve in the left plot is the result of the QCD-motivated fit described in the text. In the right plot the solid curve is approximation of the BABAR data by a smooth function, while the dotted, dash-dotted, and dashed curves represent pQCD predictions described in the text.

4. Results

The mass dependencies of the proton magnetic form factor and charged-kaon form factor below 5 GeV/c^2 are shown in Fig. 2 together with the previous measurements [5, 6, 7, 8, 9, 10, 11]. It is seen that our results are in reasonable agreement with the results from other experiments, except points marked NU [9]. These points are obtained using CLEO data collected in the maxima of the $\psi(3770)$ and $\psi(4150)$ resonances and may be shifted due to interference of resonant and nonresonant amplitudes.

In Fig. 3 we show scaled, multiplied by $M^4_{p\bar{p}}$ and $M^2_{K^+K^-}$, form factors. The curve in Fig. 3(left) is the result of a fit of the asymptotic QCD dependence of the proton form factor given by Eq. (3) to all the existing data with $M_{p\bar{p}} > 3$ GeV/c^2, excluding the two points from Ref. [9]. Our data shows that the form factor decreases in agreement with the prediction or even faster above 4.5 GeV. The points "SLAC 1993" represent data on the space-like magnetic form factor [14]. The asymptotic values of the space- and time-like form factors are expected to be the same. In the region from 3.0 to 4.5 GeV/c^2 the time-like form factor is about two-three times larger than the space-like one. The BABAR SA ISR points above 4.5 GeV/c^2 give an indication that the difference between the time- and space-like form factors decreases with mass increase.

The mass dependence of the scaled kaon form factor in Fig. 3(right) is approximated by a smooth function. The dotted curve is the asymptotic pQCD prediction for the form factor [Eq. (3)]. The dashed and dash-dotted curves represent the results of next-to-leading pQCD calculation [15] for the asymptotic (Asy) and Chernyak-Zhitnitsky (CZ) distribution amplitudes. Our data clearly indicate that the form factor decreases faster than $\alpha_s/M^2_{K^+K^-}$ approaching the pQCD predictions.

We have also measured the branching fractions:

$$\mathcal{B}(J/\psi \to p\bar{p}) = (2.33 \pm 0.08 \pm 0.09) \times 10^{-3},$$
$$\mathcal{B}(\psi(2S) \to p\bar{p}) = (3.14 \pm 0.28 \pm 0.18) \times 10^{-4},$$
$$\mathcal{B}(J/\psi \to K^+K^-) = (3.36 \pm 0.20 \pm 0.12) \times 10^{-4},$$
$$\mathcal{B}(\psi(2S) \to K^+K^-) = (0.73 \pm 0.15 \pm 0.02) \times 10^{-4},$$

which are in reasonable agreement with the PDG values [16].

References

[1] A. B. Arbuzov and T. V. Kopylova, JHEP **1204**, 009 (2012).
[2] A. Hoefer, J. Gluza and F. Jegerlehner, Eur. Phys. J. C **24**, 51 (2002).
[3] V. L. Chernyak, A. R. Zhitnitsky and V. G. Serbo, JETP Lett. **26**, 594 (1977); G. P. Lepage and S. J. Brodsky, Phys. Lett. B **87**, 359 (1979).
[4] V. L. Chernyak and A. R. Zhitnitsky, JETP Lett. **25**, 510 (1977); G. P. Lepage and S. J. Brodsky, Phys. Rev. Lett. **43**, 545 (1979).
[5] T. A. Armstrong *et al.* (E760 Collaboration), Phys. Rev. Lett. **70**, 1212 (1993).
[6] M. Ambrogiani *et al.* (E835 Collaboration), Phys. Rev. D **60**, 032002 (1999); M. Andreotti *et al.* (E835 Collaboration), Phys. Lett. B **559**, 20 (2003).
[7] M. Ablikim *et al.* (BES Collaboration), Phys. Lett. B **630**, 14 (2005).
[8] T. K. Pedlar *et al.* (CLEO Collaboration), Phys. Rev. Lett. **95**, 261803 (2005).
[9] K. K. Seth *et al.*, Phys. Rev. Lett. **110**, 022002 (2013).
[10] J. P. Lees *et al.* (BABAR Collaboration), Phys. Rev. D **87**, 092005 (2013).
[11] J. P. Lees *et al.* (BABAR Collaboration), Phys. Rev. D **88**, 032013 (2013).
[12] H. Czyz, A. Grzelinska, J. H. Kuhn and G. Rodrigo, Eur. Phys. J. C **39**, 411 (2005).
[13] J. P. Lees *et al.* (BaBar Collaboration), Phys. Rev. D **88**, 072009 (2013).
[14] A. F. Sill *et al.*, Phys. Rev. D **48**, 29 (1993).
[15] B. Melic, B. Nizic and K. Passek, Phys. Rev. D **60**, 074004 (1999).
[16] K. A. Olive *et al.* (Particle Data Group), Chin. Phys. C, **38**, 090001 (2014).